

Recurrent Distributed Reinforcement Learning for Partially Observable Robotic Assembly

Jieliang Luo, Hui Li

Autodesk Research, San Francisco, United States
 rodder.luo@autodesk.com, hui.xylo.li@autodesk.com

Abstract: In this work we solve for partially observable reinforcement learning (RL) environments by adding recurrency. We focus on partially observable robotic assembly tasks in the continuous action domain, with force/torque sensing being the only observation. We have developed a new distributed RL agent, named Recurrent Distributed DDPG (RD2), which adds a recurrent neural network layer to Ape-X DDPG [1] and makes two important improvements on prioritized experience replay [2] to stabilize training.

We demonstrate the effectiveness of RD2 on a variety of joint assembly tasks and a partially observable version of the pendulum task from OpenAI Gym. Our results show that RD2 is able to achieve better performance than Ape-X DDPG and PPO with LSTM on partially observable tasks with varying complexity. We also show that the trained models adapt well to different initial states and different types of noise injected in the simulated environment. The video presenting our experiments is available at <https://sites.google.com/view/rd2-rl>

Keywords: Robotic Assembly, Recurrent Distributed RL, Partial Observability

1 Introduction

Robotic systems for automated assembly have been widely used in manufacturing, where the environment can be carefully and precisely controlled, but they are still in infancy in architectural construction. A main reason is that current robotic systems are not adaptive to the diversity of the real world, especially in unstructured settings. RL-based robotic systems [3, 4] are a promising direction given their adaptability to uncertainties. One major challenge on this path however, is that in real-world tasks, robots often need to make decisions based on partial knowledge of the environment. For example, without the aid of a motion capture system, the pose/velocity information of objects in the environment is often unavailable or inaccurate. A vision system often fails to help due to occlusion or poor lighting conditions. Current successful RL examples require observation states to be fully observable to perform complex real-world control tasks [5, 6, 7]. However, it is unrealistic to expect a motion capture or other tracking systems at an assembly construction site as they are expensive and hard to scale.

In this paper, we present a recurrent distributed deep RL agent called Recurrent Distributed DDPG (RD2) to solve robotic assembly tasks with partial observability. Specifically, the agent can solve joint assembly tasks of varying complexity with force/torque (FT) measurements being the only observation. Similar to R2D2 [8], which extends Ape-X DQN and solves problems in the discrete action space, RD2, which solves problems in the continuous action space, introduces memory by adding an LSTM [9] layer after the first fully-connected layer in both actor and critic networks as well as their target networks. In addition, as the length of each episode in our assembly tasks is not fixed, we introduce a simple scheme to allow the overlap of the last two sequences in each episode to be variable, which maintains important information of the final transitions. Given the training instability of the DDPG family [10, 1, 11, 12], we combine the method from R2D2 to calculate priorities for each sequence and the idea of bias annealing from Schaul et al. [2] to stabilize training. Our results show that RD2 is able to achieve better performance than Ape-X DDPG and PPO [13] with LSTM (LSTM-PPO) on a partially observable pendulum task and joint assembly tasks with varying complexity. We also show that the trained policies adapt well to different initial states and different types of noise injected in the simulated environment.

We believe this work is an important step towards deploying robots on unstructured construction sites. The robots will be able to adapt to misalignment when performing assembly tasks without external tracking systems and in conditions where vision is unavailable or lighting is poor.

The remainder of this paper is structured as follows. The problem statement and related work are stated in Section 2, followed by a detailed explanation of the proposed RD2 in Section 3. Experimental setup, results, and evaluation are presented in Section 4. Section 5 concludes the paper and discusses future work.

2 Problem Statement and Related Work

2.1 Problem Statement

We model the environments in this paper as Partially Observable Markov Decision Process (POMDP), which is described by a set of states S , a set of actions A , a set of conditional probabilities $p(s_{t+1}|s_t, a_t)$ for the state transition $s_t \rightarrow s_{t+1}$, a reward function $R : S \times A \rightarrow \mathbb{R}$, a set of observations Ω , a set of conditional observation probabilities $p(o_t|s_t)$, and a discount factor $\gamma \in [0, 1]$.

In principle, the agent makes decisions based the history of observations $h_t = (o_1, a_1, o_2, a_2, \dots, o_t, a_t)$ and the goal of the agent is to learn an optimal policy π_θ in order to maximize the expected discounted rewards:

$$\max_{\pi_\theta} \mathbb{E}_{\tau \sim \pi_\theta} \left[\sum_{t=1}^T \gamma^{t-1} r(s_t, a_t) \right], \quad (1)$$

where trajectory $\tau = (s_1, o_1, a_1, s_2, o_2, a_2, \dots, s_T, o_T, a_T)$, θ is the parameterization of policy π , and $\pi_\theta(\tau) = p(s_1)p(o_1|s_1)\pi_\theta(a_1|h_1) \prod_{t=2}^T p(s_t|s_{t-1}, a_{t-1})p(o_t|s_t)\pi_\theta(a_t|h_t)$.

For many POMDP problems, it is not practical to condition on the entire history of the observations [12]. In this paper, we tackle this challenge by investigating recurrent neural networks with distributed model-free RL and we focus on the continuous action domain.

2.2 Distributed Reinforcement Learning

Distributed reinforcement learning can greatly improve sample efficiency of model-free RL by decoupling learning and data collection.

Ape-X [1] disconnects exploration from learning by having multiple actors interacting with their own environment and send the collected transitions into one of the distributed replay buffers. A learner asynchronously samples a batch of transitions from a randomly picked buffer. Ape-X has both DQN [14] and DDPG [11] variants to support discrete and continuous action spaces, respectively. Built upon Ape-X, D4PG [10] introduced a distributional critic update and incorporated N-step returns and prioritization of experience replay to achieve a more stable learning signal.

Unlike the actors and the learner in Ape-X that randomly feed and samples transitions from replay buffers, IMPALA [15] asks each actor to send the collected transitions via a first-in-first-out queue to the learner and to update its policy weights from the learner before the next episode. In addition, it introduces V-trace, a general off-policy learning algorithm that corrects a *policy-lag* between the learner and the actors as the actors' policies are usually several updates behind the learner's. Both Ape-X and IMPALA have demonstrated strong performance in the Atari-57 and DMLab-30 benchmarks, but they have not been examined on partially observable robotic assembly tasks.

2.3 RL for Robotic Assembly

RL has been studied actively in the area of robotic assembly as it can reduce human involvement and increase robustness to uncertainty. Dynamic Experience Replay [7] uses experience replay samples not only from human demonstrations but also successful transitions generated by RL agents during training and therefore improves training efficiency. Fan et al. [16] proposed a framework to combine DDPG [11] and GPS [17] to take advantage of both model-free and model-based RL [18] to solve

high-precision Lego insertion tasks. Luo et al. [19] combined iLQG [20] with FT information by incorporating an operational space controller to solve a group of high-precision assembly tasks. In our work, we only use FT measurements from the sensor mounted on the robot end-effector as the observation. This allows robots to use only their on-board low-dimensional sensor to make decisions, which improves the adaptability of the system to the diversity of the real world.

2.4 RL under Partial Observability

Partial observability is a well known challenge in robotics, resulting from occlusions, unpredictable dynamics, or noisy sensors. Hausknecht et al. [21] proposed RDQN, which replaces the first post-convolutional fully-connected layer with an LSTM layer in DQN. This modification allows the agent to only see a single frame at each timestep, but is capable of replicating DQN’s performance on standard Atari games. Built upon Ape-X DQN, Kapturowski et al. [8] extended RDQN to R2D2, where LSTM-based agents learn from distributed prioritized experience replay. The result shows that the R2D2 agent can unprecedentedly exceed human-level performance in 52 of the 57 Atari games. Because the action space of the two algorithms is discrete, they cannot address continuous control problems in robotics.

On the robotic side, OpenAI [22] used LSTM as an additional hidden layer in PPO to train a five-fingered humanoid hand to manipulate a block. The memory-augmented method was a key factor in successfully transferring the policy trained in randomized simulations to a real robotic hand, suggesting that the use of memory could help the policy to adapt to a new environment. Inoue et al. [23] used a Q-learning based method with two LSTM layers for Q-function approximation to solve low-tolerance peg-in-hole tasks. Although memory-augmented policies have proven to improve training results in continuous control problems, neither method investigated in partially observable tasks with the minimal set of observations.

3 Method

In this section, we first introduce the setup of the assembly task environment, as illustrated in Fig. 2, and then explain the details of the RD2 agent.

3.1 Assembly Tasks Setup

Observation: The observation space is 6-dimensional, being the FT measurements $(f_x, f_y, f_z, t_x, t_y, t_z)$ from the sensor, which is mounted between the last link of the robot manipulator and the parallel gripper, as shown in Fig. 2.

Action: The action space is continuous and 6-dimensional, being the desired Cartesian-space linear velocity (v_x, v_y, v_z) and angular velocity (w_x, w_y, w_z) .

Reward: We use a simple linear reward function based on the distance between the goal pose and the current pose of the moving joint member. Additionally we use a large positive reward (+100) if the current pose is within a small threshold of the goal pose:

$$r = \begin{cases} -|g - x|, & |g - x| > \epsilon \\ -|g - x| + R, & |g - x| \leq \epsilon \end{cases}$$

where x is the current pose of the joint member, g is the goal pose, ϵ is the distance threshold, and R is the large positive reward. We use the negative distance as our reward function to discourage the behavior of loitering around the goal because the negative distance also contains time penalty.

Note that this distance in the reward function currently requires a vision system or an external tracking system in the real world. However, in this paper, we focus on the recurrent distributed algorithm and experiments, assuming the reward can be learned or predicted. Existing methods [3, 24] for predicting rewards will be investigated in our future work.

Termination: An episode is terminated when the distance between the goal pose and the pose of the joint member is within a pre-defined threshold or when a pre-defined number of timesteps are reached.

3.2 The Recurrent Distributed DDPG Agent

We propose Recurrent Distributed DDPG (RD2) to study partially observable assembly tasks. Built upon Ape-X DDPG, RD2 adds an LSTM layer between the first fully-connected layer and the second fully-connected layer in both the actor and the critic networks as well as their target networks. No convolutional layers are added since we explore in the low-dimensional observation space. The details of the network architecture is provided in the Appendix A.

In the experience replay buffer, we store fixed-length sequences of transitions. Each sequence contains $(m, m=2k, \text{ where } k \in \mathbb{Z}^+)$ transitions, each of the form $(\text{observation}, \text{action}, \text{reward})$. Adjacent sequences overlap by $m/2$ timesteps and the batches of sequences never cross the episode boundary. As the length of the episodes in our assembly tasks varies, we introduce a dynamic mechanism to allow the last overlap in each episode to be a variable between $[m/2, m - 1]$. Specifically, the last overlap is calculated as:

$$O = \begin{cases} m - T \bmod (m/2), & T \bmod (m/2) \neq 0 \\ m/2, & T \bmod (m/2) = 0 \end{cases}$$

where O is the number of transitions in the last overlap and T is the total timesteps in each episode. This mechanism prevents losing or compromising any transitions at the end of each episode, which usually contain crucial information for training.

Similar to R2D2, we sample the sequences in the replay buffer based on their priorities, formulated as:

$$p = \eta \max(\delta) + (1 - \eta)\bar{\delta}$$

where δ is a list of absolute n-step TD-errors in one sequence. We set η to 0.9 to avoid compressing the range of priorities and limiting the ability to pick out useful experience.

In addition, as discussed in [2], prioritized replay introduces bias because it changes the distribution of the stochastic updates in an uncontrolled fashion, and therefore changes the solution that the estimates converge to. For each transition in a sequence, we correct the bias using importance-sampling weights

$$w_i = (N \times P(i))^{-\beta}$$

where N is the size of the replay buffer and we set β to 0.4. We normalize the weight of each transition before sending the sequences for backpropagation through time (BPTT) [25] by $1/\max_i w_i$. On the implementation level, we initialize two sum-tree data structures such that one keeps the priorities of the sequences and the other one keeps the priorities of the transitions. We observe that this step is crucial to stabilize the training process for our tasks.

We use a zero start state in LSTM to initialize the network at the beginning of the sampled sequence and train the RD2 agent with Population Based Training (PBT) [26] on an AWS p3.16xlarge instance. Every training session includes 8 concurrent trials, each of which contains one single GPU-based learner and 8 workers. We make the size of the batches, the length of the sequences, and n-step as mutable hyper-parameters to PBT. Each trial evaluates in every 5 iterations to determine whether to keep the current training or copy from a better trial. If a copy happens, the mutable hyper-parameters are perturbed by a factor of 1.2 or 0.8 or have 25% probability to be re-sampled from the original distribution. The details of the hyper-parameters fine-tuned in PBT are provided in Table 1 below.

4 Experiments

In this section, we compare the performance of RD2 with two algorithms: Ape-X DDPG and LSTM-PPO, which are also trained with PBT with 8 concurrent trials, each of which contains one single GPU-based learner and 8 workers. Their fine-tuned hyperparameters in PBT are listed in Appendix B. Sec. 4.1 compares the algorithms on the Pendulum benchmark problem and its partially observable version. In Sec. 4.2 we introduce a customized joint assembly environment and compare the

Fine-tuned Hyperparameter	Fine-tuned range
Number of batches	(20, 120) ¹
Sequence length	[16, 32, 64, 128] ²
Target network update frequency	[25000, 50000, 75000, 100000]
N-step	(3, 8)
Minimal iteration time (s)	[30, 40, 50, 60]

¹ Sampled from the given range, ² Sampled from the given list

Table 1: The hyper-parameters fine-tuned in RD2 using PBT

algorithms on eight different tasks. Sec. 4.3 evaluates the adaptability of trained policies to initial offsets and noise injected in simulation. The video presenting our experiments is available at <https://sites.google.com/view/rd2-rl>

4.1 Pendulum Tasks

We compare RD2’s performance on the pendulum task from OpenAI Gym [27] and its partially observable version that only takes the joint angle $[\cos(\theta), \sin(\theta)]$ as observation. The results of the two tasks are shown in Fig 1, showing that RD2 performs slightly worse than the other two algorithms on the fully observable pendulum task, but significantly improves the performance on the the partially observable version, which both Ape-X DDPG and LSTM-PPO fail at.

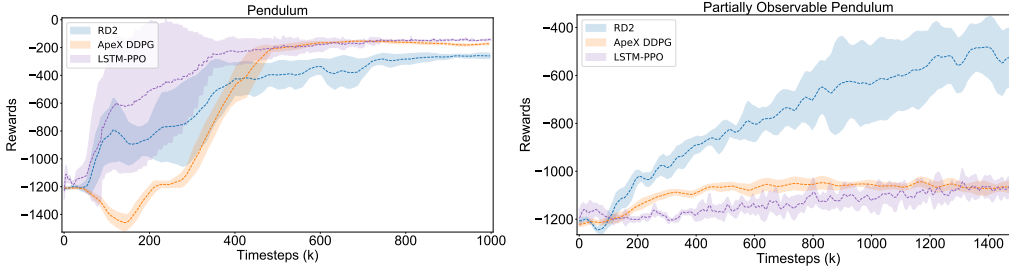


Figure 1: Reward comparison for the pendulum task and its partially observable version. The dotted lines visualize the average of the best model performance across time for three PBT runs with different random seeds and the shaded areas show the 95% confidence bound.

4.2 Joint Assembly Tasks

We further compare RD2’s performance in a joint assembly environment built in the PyBullet [28] simulation engine. The environment consists of two Franka Panda robotic arms, each of which holds a member of the joint and the two members are perpendicular to each other by default, as shown in Fig. 2. One arm is fixed and keeping a joint member static. The other arm moves the other joint member to complete the joint. We have 8 tasks in the environment with varying complexity, by setting the fixed arm at different initial poses. In effect, the joint member on the fixed arm either has an angular offset or a linear offset from its default pose. In general, the larger the offset or the more axes are involved, the more difficult it is to train. Table 2 describes the details of each task. We present these tasks because harder tasks result in failure among all three algorithms, and hence are not meaningful.

Angular Offset	Termination	Position Offset	Termination
No offset	1M timesteps	10mm on Y axis	3M timesteps
2 degree around XYZ axes	5M timesteps	10mm on XY axes	3M timesteps
4 degree around XY axes	5M timesteps	5mm on XYZ axes	3M timesteps
8 degree around X axis	5M timesteps	10mm on XYZ axes	3M timesteps

Table 2: The eight tasks to evaluate RD2 on joint assembly with varying initial offsets.

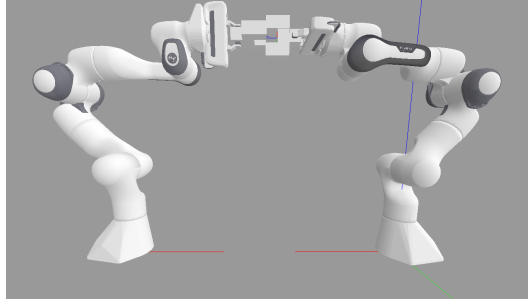


Figure 2: The joint assembly environment in PyBullet. The robot arm on the left is fixed in position and orientation. The robot arm on the right assembles the joint based on FT measurements only.

The results of the four angular-offset tasks and the four linear position-offset tasks are shown in Fig 3 and Fig 4 respectively. Both figures show that RD2 has the best performance across all tasks. In easier tasks, like no offset, 2 degree angular offset around XYZ axes, and 5mm linear offset on XYZ axes, the advantage of RD2 is minor. However, RD2 can remarkably improve performance on harder tasks, like 4 degree angular offset around XZ axes or 8 degree angular offset around X axis, which cannot be solved by either Ape-X DDPG or LSTM-PPO. Both memory-augmented algorithms, RD2 and LSTM-PPO, show strength on harder tasks. Although LSTM-PPO has relatively more stable learning curves, it is unable to achieve the optimal policies achieved by RD2 in the given timesteps.

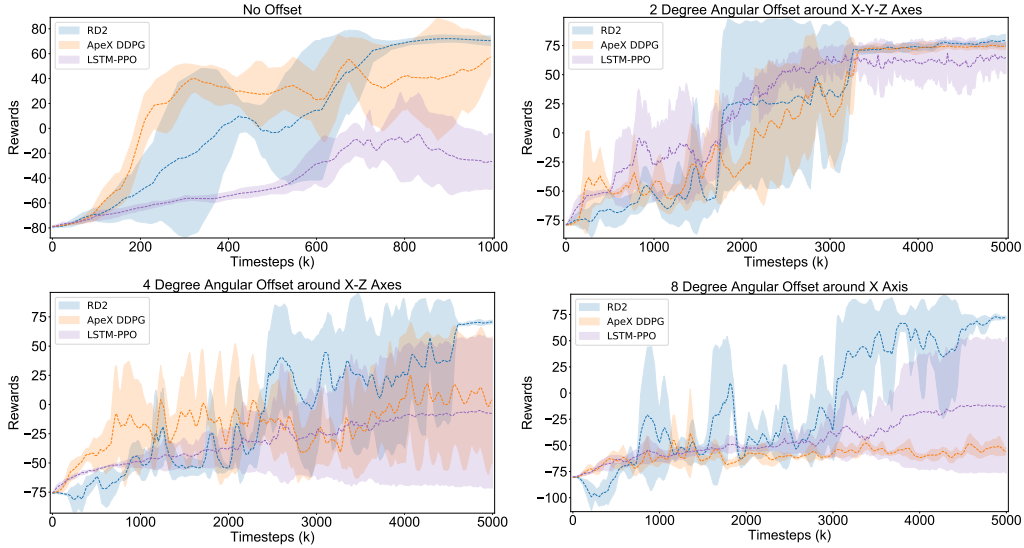


Figure 3: Rewards comparison for the four angular offset experiments. The dotted lines visualize the average of the best model performance across time for three PBT runs with different random seeds and the shaded areas show the 95% confidence bound.

4.3 Evaluation of Adaptation

In this section, we evaluate how well the trained policies adapt to new situations. We specifically consider two types of situations. One is initial offsets, which are initial positions or initial orientations that deviate from those in training. The other is physical noise in simulation, such as FT sensor noise and inaccuracy in friction modeling. We use two trained policies and run 20 rollouts for each case.

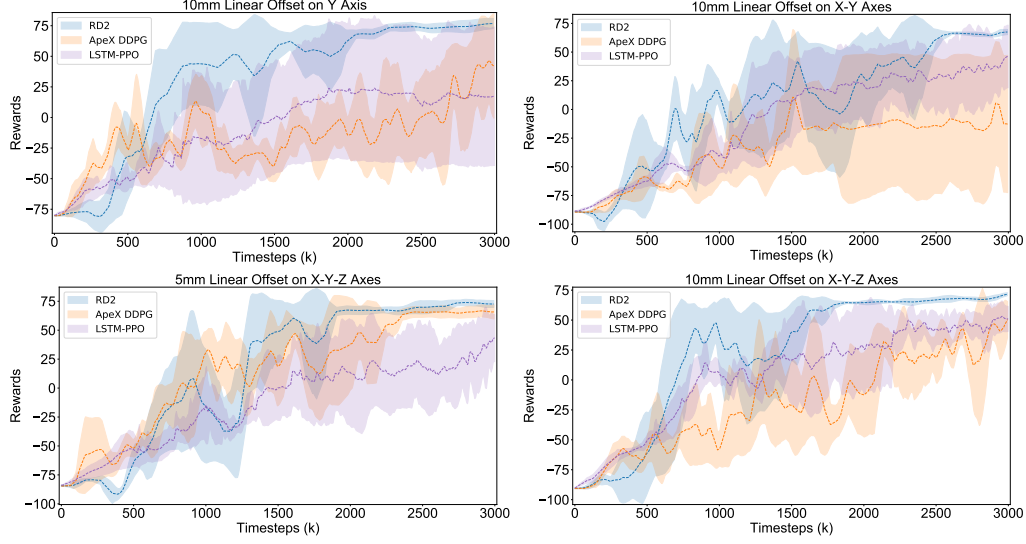


Figure 4: Reward comparison for the four linear position offset experiments. The dotted lines visualize the average of the best model performance across time for three PBT runs with different random seeds and the shaded areas show the 95% confidence bound.

4.3.1 Initial Pose Offset

Real-world robotic assembly tasks often require the system to be adaptable to small misalignment or errors, as rarely can the initial condition be exactly as planned in the real world. In a joint assembly task, small misalignment is often unavoidable due to fabrication tolerance or material deflection.

We evaluate the adaptability of trained policies with varying initial positional offset and angular offset. As shown in Fig. 5 left, our policy adapts well to linear offsets $\leq 10\text{mm}$ in three axes. 100% success rate is achieved on both the 5mm and 10mm offset tasks, although because 10mm on all axes is not a small misalignment, the mean reward for the task is lower. As shown in Fig. 5 right, our trained policy adapts well to isolated and small angular offsets, such as 5 degrees around Y and 2 degrees around Z, with success rate both at 100%. When there is an offset around two or more axes, the mean reward is lower and the success rate reduces to 55%.

One thing to note is the issue of overfitting. During training, when the termination condition is set to very high average reward, which translates to near 100% success rate across episodes, the trained policy adapts poorly to even small offsets during evaluation. To avoid overfitting and increase adaptability, we recommend lowering the target average reward by 10 – 15% to balance between overfitting and underfitting.

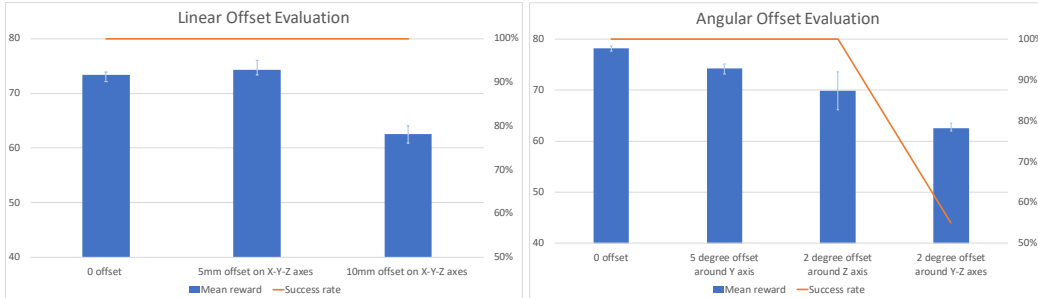


Figure 5: Results of the linear offset evaluation (left) and the angular offset evaluation (right). There are 20 runs in each evaluation case. Each blue bar indicates the mean reward of the successful runs and each error bar indicates the max and min reward in the successful runs. The orange line reflects the success rates across all the evaluation cases. The Y axis of the plot on the left indicates the reward and on the right indicates the success rate.

4.3.2 Physical Noise in Simulation

From our past experiments with real hardware, we learned that FT sensor noise in the real world and inaccurate modeling of friction in simulation are the two main contributors to the sim-to-real gap for robotic assembly. Hence, as an effort to evaluate how well our simulation-trained policy can transfer to the real world, we inject noise in simulation during the evaluation phase. More specifically, we add Gaussian noise in the FT observation and in the friction parameter in simulation.

For the FT observation, we add 0-mean Gaussian noise with standard deviation of 50% and 80% of the nominal FT value during evaluation. As shown in Fig. 6, our trained policy adapts well to the 50% standard deviation, with success rate at 90%. As the FT noise standard deviation increases to 80%, the mean reward of the policy lowers and its success rate reduces 50%. For the friction parameter, we add 0-mean Gaussian noise with standard deviation of 100% of the nominal friction value during evaluation. As shown in Fig. 6, the trained policy adapts well by maintaining similar mean reward to that without any noise and having slightly lower success rate, at 80%. When both types of noise are combined, the success rate and mean reward are slightly lowered.

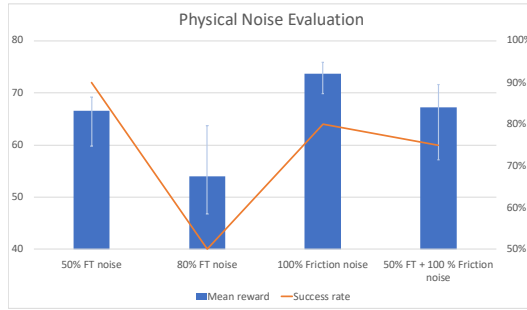


Figure 6: Results of the physical noise evaluation. There are 20 runs in each evaluation case. Each blue bar graph indicates the mean reward of the successful runs and each error bar indicates the max and min reward in the successful runs. The orange line reflects the success rates across all the evaluation cases. The Y axis of the plot on the left indicates the reward and on the right indicates the success rate.

5 Discussion and Future Work

This paper introduced a distributed RL agent called Recurrent Distributed DDPG (RD2) to solve partially observable robotic assembly tasks with FT measurements being the only observation. Inspired by R2D2, RD2 introduces recurrency in Ape-X DDPG, but this single adjustment is not sufficient to solve our proposed tasks due to instability of the DDPG family. We developed two improvements on prioritized experience replay as discussed in Section 3.2 to stabilize the performance of RD2.

We show that RD2 achieves the best performance on all assembly tasks in comparison to Ape-X DDPG and LSTM-PPO. We observe that RD2 has minor advantages on easy assembly tasks but demonstrates its strength on difficult tasks that cannot be solved by either of the other two algorithms. We also show that our trained policies adapt well to various initial pose misalignment as well as physical noise injected in simulation.

In the future, we would like to evaluate RD2 on a larger variety of assembly tasks to understand its full scope. We would also like to remove distance from the reward function as the next step to enable real robots to perform complex assembly tasks in unstructured settings with minimal on-board sensors.

Acknowledgments

We thank Tonya Custis and Erin Bradner for budgetary support of the project; Richard Liaw for technical support.

A Specification of the neural networks used in RD2

Layer	Input Size	Output Size
Fully-connected (Relu)	[#Observations]	[256]
LSTM (Relu)	[256]	[256]
Fully-connected (Q Network)	[256]	[1]
Fully-connected (Tanh) (π Network)	[256]	[#Actions]

Table 3: Specification of the Q network and π network used in RD2 for all the experiments. It also applies to their target networks.

B Hyperparameters fine-tuned in PBT

Ape-X DDPG: target network update frequency, replay buffer size, sample batch size, train batch size, and minimal iteration time(s).

LSTM-PPO: number of SGD iterations, SGD minibatch size, train batch size, learning rate, and value function loss coefficient.

References

- [1] D. Horgan, J. Quan, D. Budden, G. Barth-Maron, M. Hessel, H. Van Hasselt, and D. Silver. Distributed prioritized experience replay. *arXiv preprint arXiv:1803.00933*, 2018.
- [2] T. Schaul, J. Quan, I. Antonoglou, and D. Silver. Prioritized experience replay. *arXiv preprint arXiv:1511.05952*, 2015.
- [3] H. Zhu, J. Yu, A. Gupta, D. Shah, K. Hartikainen, A. Singh, V. Kumar, and S. Levine. The ingredients of real-world robotic reinforcement learning. *arXiv preprint arXiv:2004.12570*, 2020.
- [4] O. M. Andrychowicz, B. Baker, M. Chociej, R. Jozefowicz, B. McGrew, J. Pachocki, A. Petron, M. Plappert, G. Powell, A. Ray, et al. Learning dexterous in-hand manipulation. *The International Journal of Robotics Research*, 39(1):3–20, 2020.
- [5] G. Schoettler, A. Nair, J. Luo, S. Bahl, J. A. Ojea, E. Solowjow, and S. Levine. Deep reinforcement learning for industrial insertion tasks with visual inputs and natural rewards. *arXiv preprint arXiv:1906.05841*, 2019.
- [6] I. Akkaya, M. Andrychowicz, M. Chociej, M. Litwin, B. McGrew, A. Petron, A. Paino, M. Plappert, G. Powell, R. Ribas, et al. Solving rubik’s cube with a robot hand. *arXiv preprint arXiv:1910.07113*, 2019.
- [7] J. Luo and H. Li. Dynamic experience replay. *arXiv preprint arXiv:2003.02372*, 2020.
- [8] S. Kapturowski, G. Ostrovski, J. Quan, R. Munos, and W. Dabney. Recurrent experience replay in distributed reinforcement learning. In *International conference on learning representations*, 2018.
- [9] S. Hochreiter and J. Schmidhuber. Long short-term memory. *Neural computation*, 9(8):1735–1780, 1997.
- [10] G. Barth-Maron, M. W. Hoffman, D. Budden, W. Dabney, D. Horgan, A. Muldal, N. Heess, and T. Lillicrap. Distributed distributional deterministic policy gradients. In *6th International Conference on Learning Representations*, 2018.

- [11] T. P. Lillicrap, J. J. Hunt, A. Pritzel, N. Heess, T. Erez, Y. Tassa, D. Silver, and D. Wierstra. Continuous control with deep reinforcement learning. In *6th International Conference on Learning Representations*, 2016.
- [12] N. Heess, J. J. Hunt, T. P. Lillicrap, and D. Silver. Memory-based control with recurrent neural networks. *arXiv preprint arXiv:1512.04455*, 2015.
- [13] J. Schulman, F. Wolski, P. Dhariwal, A. Radford, and O. Klimov. Proximal policy optimization algorithms. *arXiv preprint arXiv:1707.06347*, 2017.
- [14] V. Mnih, K. Kavukcuoglu, D. Silver, A. A. Rusu, J. Veness, M. G. Bellemare, A. Graves, M. Riedmiller, A. K. Fidjeland, G. Ostrovski, et al. Human-level control through deep reinforcement learning. *Nature* 518, pages 529–533, 2015.
- [15] L. Espeholt, H. Soyer, R. Munos, K. Simonyan, V. Mnih, T. Ward, Y. Doron, V. Firoiu, T. Harley, I. Dunning, et al. Impala: Scalable distributed deep-rl with importance weighted actor-learner architectures. *arXiv preprint arXiv:1802.01561*, 2018.
- [16] Y. Fan, J. Luo, and M. Tomizuka. A learning framework for high precision industrial assembly. *arXiv preprint arXiv:1809.08548v3*, 2018.
- [17] S. Levine and V. Koltun. Guided policy search. In *International Conference on Machine Learning*, pages 1–9, 2013.
- [18] R. S. Sutton and A. G. Barto. *Reinforcement learning: An introduction*. MIT press, 2018.
- [19] J. Luo, E. Solowjow, C. Wen, J. A. Ojea, A. M. Agogino, A. Tamar, and P. Abbeel. Reinforcement learning on variable impedance controller for high-precision robotic assembly. *arXiv preprint arXiv:1903.01066*, 2019.
- [20] E. Todorov and W. Li. A generalized iterative lqg method for locally-optimal feedback control of constrained nonlinear stochastic systems. In *Proceedings of the 2005, American Control Conference, 2005.*, pages 300–306. IEEE, 2005.
- [21] M. Hausknecht and P. Stone. Deep recurrent q-learning for partially observable mdps. In *2015 AAAI Fall Symposium Series*, 2015.
- [22] OpenAI, M. Andrychowicz, B. Baker, M. Chociej, R. Józefowicz, B. McGrew, J. Pachocki, A. Petron, M. Plappert, G. Powell, A. Ray, J. Schneider, S. Sidor, J. Tobin, P. Welinder, L. Weng, and W. Zaremba. Learning dexterous in-hand manipulation. *CoRR*, 2018. URL <http://arxiv.org/abs/1808.00177>.
- [23] T. Inoue, G. De Magistris, A. Munawar, T. Yokoya, and R. Tachibana. Deep reinforcement learning for high precision assembly tasks. In *2017 IEEE/RSJ International Conference on Intelligent Robots and Systems (IROS)*, pages 819–825. IEEE, 2017.
- [24] M. Okada, N. Kosaka, and T. Taniguchi. Planet of the bayesians: Reconsidering and improving deep planning network by incorporating bayesian inference. *arXiv preprint arXiv:2003.00370*, 2020.
- [25] P. J. Werbos. Backpropagation through time: what it does and how to do it. *Proceedings of the IEEE*, 78(10):1550–1560, 1990.
- [26] M. Jaderberg, V. Dalibard, S. Osindero, W. M. Czarnecki, J. Donahue, A. Razavi, O. Vinyals, T. Green, I. Dunning, K. Simonyan, et al. Population based training of neural networks. *arXiv preprint arXiv:1711.09846*, 2017.
- [27] G. Brockman, V. Cheung, L. Pettersson, J. Schneider, J. Schulman, J. Tang, and W. Zaremba. Openai gym. *arXiv preprint arXiv:1606.01540*, 2016.
- [28] E. Coumans and Y. Bai. Pybullet, a python module for physics simulation for games, robotics and machine learning. *GitHub repository*, 2016.